Wydawnictwo UR 2024
ISSN 2544-1361 (online)
doi: 10.15584/ejcem.2024.2.25

http://www.ejcem.ur.edu.pl
European Journal of Clinical and Experimental Medicine
Eur J Clin Exp Med 2024; 22 (2): 376–387

ORIGINAL PAPER

Synthesis, characterization of isoxazole derivatives and evaluation of their antibacterial, antioxidant and anticancer activity

Ketan Vashisht [1], Pooja Sethi [1], Anshul Bansal [2], Tejveer Singh [3], Raman Kumar [4], Hardeep Singh Tuli [4], Shallu Saini [4]

[1] Department of Chemistry, M.M. Engineering College, Maharishi Markandeshwar (Deemed to be University), Mullana, Haryana, India
[2] Department of Chemistry, S.A. Jain College, Ambala, Haryana, India
[3] Translational Oncology Laboratory, Department of Zoology, Hansraj College, University of Delhi, India
[4] Department of Bio-Sciences and Technology, M.M. Engineering College, Maharishi Markandeshwar (Deemed to be University), Mullana, Haryana, India

ABSTRACT

Introduction and aim. The synthesis of heterocyclic compounds containing oxygen and nitrogen is profoundly intriguing due to their mechanistic implications in both research and development within organic chemistry and drug discovery. The primary aim of this study is to fabricate a range of pharmacologically active drugs containing the isoxazole moiety.

Material and methods. The synthesis of new derivatives of isoxazole was achieved through a one-pot condensation reaction of 2-[(Substituted phenyl)hydrazono]malononitrile (1) and 3-[(Substituted phenyl)azo]-2,4-Pentanedione (2) with sodium acetate and hydroxylamine hydrochloride (1:1) in ethanol. All the compounds were screened for their *in vitro* antibacterial activity, in vitro antioxidant and anticancer activity. The synthesized compounds underwent characterization through FTIR, ^{1}H NMR, and ^{13}C NMR analyses, supported by mass spectral data and elemental analysis.

Results. A set of novel isoxazole derivatives was synthesized with a favorable yield. Among compounds 1d, 1e, 2c, 2d, and 2e exhibited notable antioxidant activities. Compounds 1a, 1b, and 1c demonstrated significant anticancer potential against prostate cancer [PC3] cell lines compared to normal HEK cell lines, while 2a displayed the highest inhibitory zone against *Escherichia coli*.

Conclusion. Novel compounds with multifaceted biological activities have been successfully designed, and a synthetic route to create isoxazole derivatives has been devised and verified.

Keywords. antibacterial, antioxidant activity and anticancer potential, isoxazole, pathogenic bacterial

Introduction

For researchers worldwide, addressing bacterial infectious diseases remains an extremely vital and challenging issue.[1] Despite the invention of numerous novel antimicrobial drugs, their clinical efficacy remains limited in treating a growing number of life-threatening viral infections. This limitation arises from their high toxicity risk and the potential for developing drug resistance through gene sequence alterations.[2-3]

Isoxazole, along with numerous other heterocyclic compounds, holds a broad spectrum of pharmaceutical applications (Fig. 1).

Corresponding author: Pooja Sethi, e-mail: sethipuja1001@gmail.com, pooja.amb80@gmail.com, poojachem@mmumullana.org

Received: 7.12.2023 / Revised: 8.02.2024 / Accepted: 13.02.2024 / Published: 30.06.2024

Vashisht K, Sethi P, Bansal A, Singh T, Kumar R, Tuli HS, Saini S. Synthesis, characterization of isoxazole derivatives and evaluation of their antibacterial, antioxidant and anticancer activity. *Eur J Clin Exp Med.* 2024;22(2):376–387. doi: 10.15584/ejcem.2024.2.25.

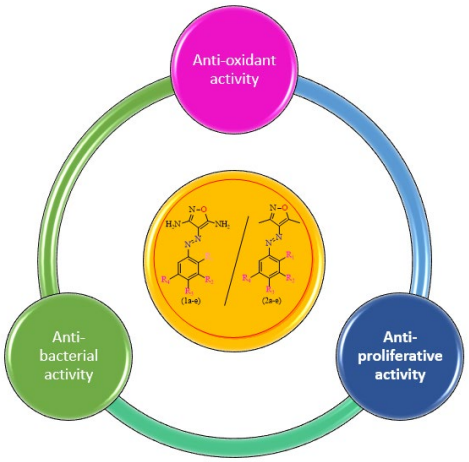

Fig. 1. Graphical abstract depicting the activity of isoxazole compounds

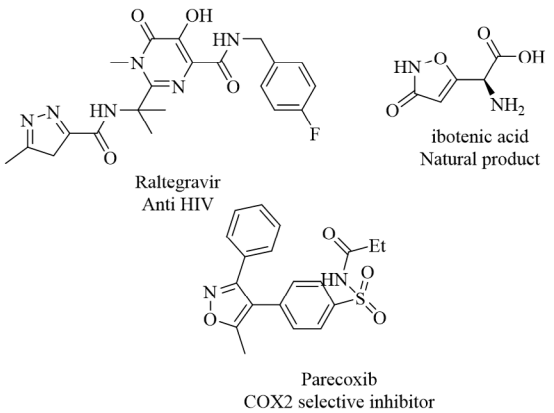

Fig. 2. Isoxazole contained drug

Exploring techniques for the development and synthesis of various heterocyclic-containing isoxazole scaffolds and their applications holds great importance in the realm of medicinal chemistry. Heterocyclic compounds, including isoxazole, are meticulously examined for their pharmacological actions and have emerged as significant pharmacophores.[4-6] These compounds exhibit a wide range of therapeutic uses, including anti-inflammatory effects, CNS depressant properties, antimicrobial activity, analgesic effects, anti-cancer properties, antioxidant properties, anti-tubercular activity, and various other biological activities such as GABA (γ-aminobutyric acid) agonistic activity, antihypertensive activity, and inhibitory activity.[7-23] Isoxazole plays a crucial role in synthesizing numerous natural and artificial compounds. Additionally, researchers have demonstrated various biological activities of different types of azole-based heterocyclic compounds, underscoring their medicinal significance (Fig. 2). The presence of diverse functional groups, such as amides, azoles, and alkyl groups, linked to the basic pharmacophoric unit structure, results in different modes of action that may be beneficial for treating microbial infections.[24]

Based on these observations and our work related to isoxazole synthesis, spectroscopy, and biological studies, this study aimed to evaluate the antioxidant, anti-cancer, and antibacterial activities of a series of novel isoxazole compounds.

Aim

In this research article, we conducted the synthesis of isoxazole derivatives and evaluated the antibacterial, antioxidant and anticancer activities of a series of novel isoxazole compounds.

Material and methods

Thin layer chromatography (TLC) was employed to ensure the completeness and purity of the reactions. Infrared (IR) spectra were acquired using a DRS probe on a SHIMADZU-FTIR-8400 spectrophotometer, covering frequencies ranging from 4000 to 400 cm^{-1}. NMR spectra were recorded on a BRUKER AVANCE II spectrometer at 500 MHz for both ^{1}H and ^{13}C nuclei, with DMSO-d6 serving as the solvent and TMS as the internal standard. Mass spectra were obtained using a direct intake probe on the mass spectrometer. Compounds utilized in this study were provided by Merck and Spectrochem Chemical companies, and all obtained compounds were of reagent grade. Additionally, all solvents were freshly distilled prior to use.

Experimental section

General protocol for the synthesis of hydrazone 2-[(Substituted Phenyl)hydrazono]malononitrile (1) (SMN) and 3-(substituted phenylazo)-2,4-pentanedione (2) (SPD)

The diazotization of various *-o*, *-m*, *-p*-substituted anilines is followed by *in situ* condensation with malononitrile and acetylacetone in the presence of sodium acetate, yielding the intermediates 2-[(substituted phenyl)hydrazono]malononitrile (1) (SMN) and 3-(substituted phenylazo)-2,4-pentanedione (2) (SPD). Diazotization is a process wherein an amine group ($-NH_2$) is converted into a diazonium salt by treatment with sodium nitrite ($NaNO_2$). After diazotization, the diazonium salt reacts with malononitrile (cyanoacetic acid) within the same reaction vessel. In a separate step, the diazonium salt reacts with acetylacetone (also known as 2,4-pentanedione). Both end products, 2-[(substituted phenyl) hydrazono]malononitrile (1) (SMN) and 3-(substituted phenylazo)-2,4-pentanedione (2) (SPD), serve as versatile intermediates that can be utilized in other synthetic transformations to generate alternative compounds with desired properties.[25]

General process for the synthesis of isoxazole (1a-e) and (2a-e)

Furthermore, treatment of 2-[(substituted phenyl)hydrazono]malononitrile (SMN) (1) (0.94 g, 5 mmol) and

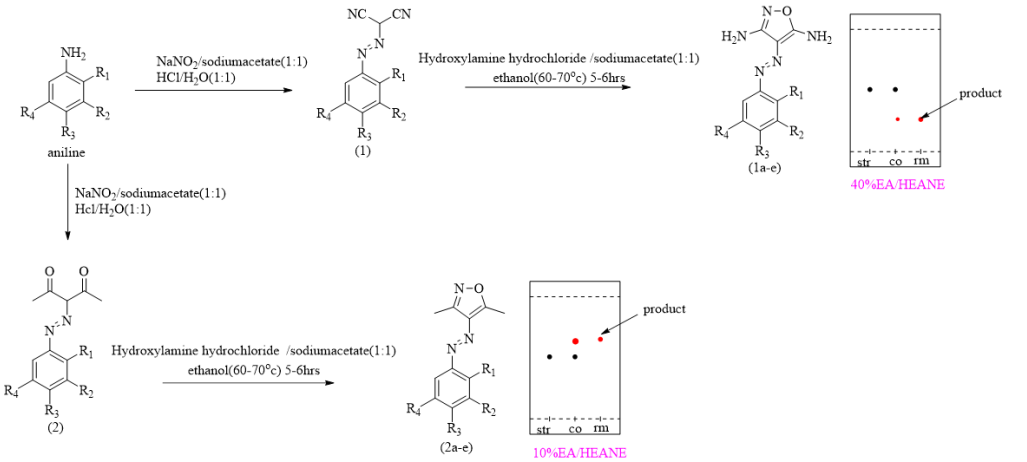

Fig. 3. Synthesis of compound (1a-e) and (2a-e)

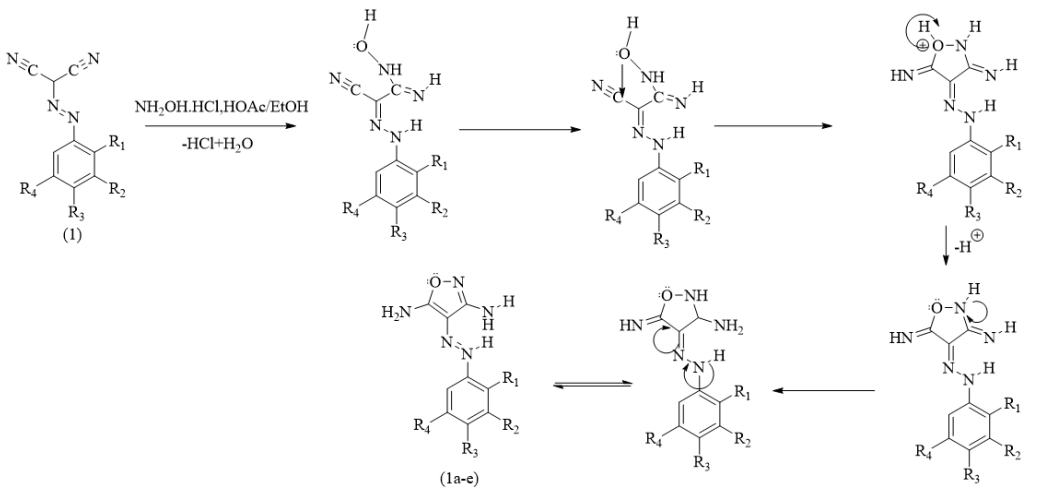

Fig. 4. Mechanism of synthetic path of compounds (1a-e)

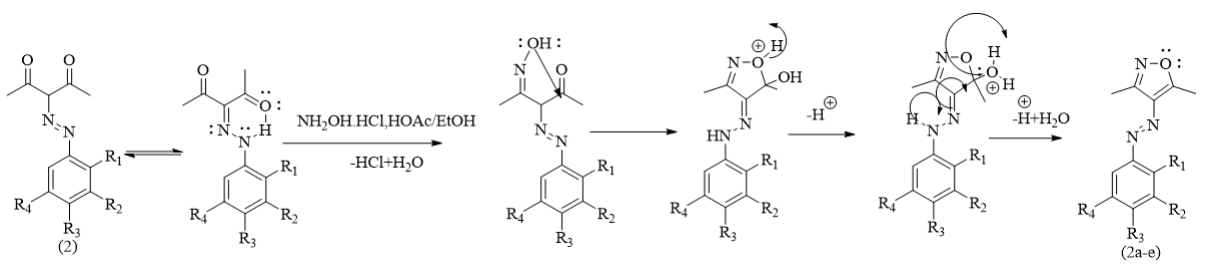

Fig. 5. Mechanism of synthetic path of compounds (2a-e)

3-(substituted phenylazo)-2,4-pentanedione (SPD) (2) (5 mmol) with hydroxylamine hydrochloride and sodium acetate (1:1) in refluxing ethanol yielded compounds (1a-e) and (2a-e) as exclusive products (Fig. 3). The reaction mixture was stirred for 5-6 hours at 60–70°C and monitored by TLC. Upon completion, the reaction was quenched with ice-cold water. The crude product (15 mL) was then extracted with chloroform, and the organic layer was washed with water before being evaporated in a rotary evaporator to obtain the solid component. Subsequently, the product underwent recrystallization in ethanol for purification. The physicochemical characterization is presented in Table 1, and Figure 4 and 5 illustrate the synthesis mechanisms.

3,5-Diamino-4-(4'-bromophenylazo) isoxazole (1a) (Fig. 6)

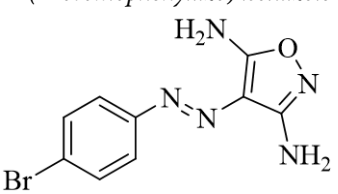

Fig. 6. 3,5-Diamino-4-(4'-bromophenylazo) isoxazole (1a)

Yield: 81%; IR (ν_{max},cm^{-1}): 3420, 3234(NH_2), 1610(C=C), 1391(N=N), 616(C-Br); (IR spectrum of compound in Figure S1); ^{1}H NMR (500 MHz, DMSO-d6) δ 7.61(d, 2H), 7.72 (d,2H), 6.15(s, 2H, D_2O exchangeable), 8.32(s, 2H, D_2O exchangeable), ^{13}C NMR (500 MHz, DMSO) δ 105.11, 120.25, 122.66, 131.14, 131.70, 150.12, 151.86, MS (EI): $[M+1]^+$ and $[M+1+2]^+$ 283.96, 284.96. Anal. Calcd. For $C_9H_8BrN_5O$: C, 38.32; H, 2.86; N, 24.83; Found: C, 38.31; H, 2.85; N, 24.79. (^{1}H-NMR data is shown in Figure S11, ^{13}C- NMR data is shown in Figure S21, D_2O exchange data shown in Figure S26, mass spectrum in Figure S28 and elemental analysis shown in Figure S33).

3,5-Diamino-4-(3'-chlorophenylazo) isoxazole (1b) (Fig. 7)

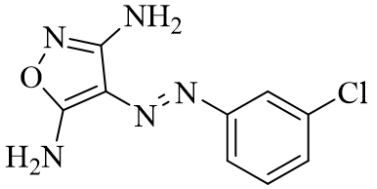

Fig. 7. 3,5-Diamino-4-(3'-chlorophenylazo) isoxazole (1b)

Yield: 85%; IR (ν_{max},cm^{-1}): 3408, 3242(NH_2), 1625(C=C), 1370(N=N), 631(C-Cl); (IR spectrum of compound in Figure S2); ^{1}H NMR (500 MHz, DMSO-d6) δ 7.87(s,1H), 7.72 (d,1H), 7.48(d,1H), 7.3(dd,1H), 6.25(s, 2H, D_2O exchangeable), 8.41(s, 2H, D_2O exchangeable), ^{13}C NMR(500 MHz, DMSO) δ 107.14, 126.92, 128.81, 129.11, 130.08, 130.24, 132.24, 155.12, 161.9, MS(EI): $[M+1]^+$ and $[M+1+2]^+$, m/z, 238.95, 239.95. Anal. Calcd. For $C_9H_8ClN_5O$: C, 45.49; H, 3.39; N, 29.47; Found: C, 46.12; H, 3.05; N, 29.14 (^{1}H-NMR data is shown in Figure S12).

3,5-Diamino-4-(4'-fluorophenylazo) isoxazole (1c) (Fig. 8)

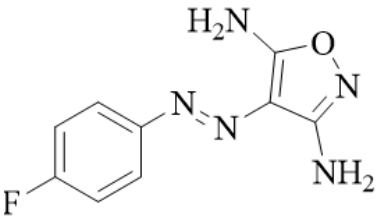

Fig. 8. 3,5-Diamino-4-(4'-fluorophenylazo) isoxazole (1c)

Yield: 82%; IR (ν_{max},cm^{-1}): 3420, 3242(NH_2), 1610(C=C), 1395(N=N), 609(C-F); (IR spectrum of compound in Figure S3); ^{1}H NMR(500 MHz, DMSO-d6) δ 7.80(d, 2H), 7.26 (d,2H), 6.11(s, 2H, D_2O exchangeable), 8.29(s, 2H, D_2O exchangeable), ^{13}C NMR (500 MHz, DMSO) δ 107.62, 115.58, 116.10, 116.27, 122.48, 149.55, 162.48 MS(EI):$[M+1]^+$, m/z, 221.09. Anal. Calcd. For $C_9H_8FN_5O$: C, 48.87; H, 3.65; N, 31.66; Found: C, 48.42; H, 3.55; N, 30.92. (^{1}H-NMR data is shown in Figure S13, ^{13}C- NMR data is shown in Figure S22, D_2O exchange data shown in Figure S27, mass spectrum in Figure S29).

3,5-Diamino-4-(2'-bromophenylazo) isoxazole (1d) (Fig. 9)

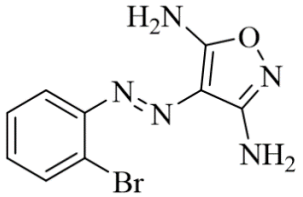

Fig. 9. 3,5-Diamino-4-(2'-bromophenylazo) isoxazole (1d)

Yield: 78%; IR (ν_{max},cm^{-1}): 3397, 3234 (NH_2), 1618 (C=C), 1469(N=N), 624(C-Br); (IR spectrum of compound in Figure S4); ^{1}H NMR(500 MHz, DMSO-d6) δ 7.81(d, 1H), 7.72 (dd,1H), 7.58(dd,1H), 7.20(d,1H), 6.45(s, 2H, D_2O exchangeable), 8.51(s, 2H, D_2O exchangeable), ^{13}C NMR (500 MHz, DMSO) δ 102.52, 117.41, 127.71, 128.12, 131.0, 131.6, 131.9, 150.21, 158.9, MS (EI): $[M+1]^+$ and $[M+1+2]^+$, 283.96, 284.96. Anal. Calcd. For $C_9H_8BrN_5O$: C, 38.32; H, 2.86; N, 24.83; Found: C, 38.24; H, 2.91; N, 24.72. (^{1}H-NMR data is shown in Figure S14 and elemental analysis shown in Figure S34).

3,5-Diamino-4-(2'-chlorophenylazo) isoxazole (1e) (Fig. 10)

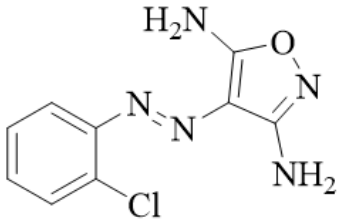

Fig. 10. 3,5-Diamino-4-(2'-chlorophenylazo) isoxazole (1e)

Yield: 81%; IR (ν_{max},cm^{-1}): 3412, 3264 (NH_2), 1632 (C=C), 1506(N=N), 602(C-Cl); (IR spectrum of compound in Figure S5); ^{1}H NMR(500 MHz, DMSO-d6) δ 7.81(d,1H), 7.72(dd,1H), 7.57(dd,1H), 7.28(d,1H), 6.43(s, 2H, D_2Oexchangeable), 8.50(s, 2H, D_2O exchangeable), ^{13}C NMR(500 MHz, DMSO) δ 105.12, 126.81, 128.47, 128.88, 130.29, 130.34, 134.37, 152.21, 158.91, MS(EI): $[M+1]^+$and $[M+1+2]^+$, m/z, 238.95, 239.95. Anal. Calcd. For $C_9H_8ClN_5O$: C, 45.49; H, 3.39; N, 29.47; Found: C, 45.92; H, 3.35; N, 29.24. (^{1}H-NMR data is shown in Figure S15).

3,5-Dimethyl-4-(2'-chloro-4'-nitrophenylazo) isoxazole (2a) (Fig. 11)

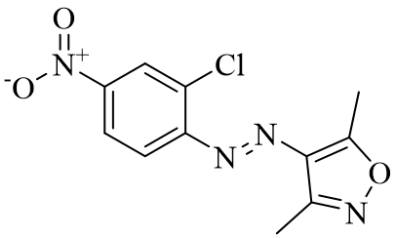

Fig. 11. 3,5-Dimethyl-4-(2'-chloro-4'-nitrophenylazo) isoxazole (2a)

Yield: 91%; IR (ν_{max},cm^{-1}): 2915, 2896(C-H), 1610 (N=N), 1545(C=C), 1403(N-O), 672(C-Cl); (IR spectrum of compound in Figure S6); ^{1}H NMR(500 MHz, DMSO-d6) δ 2.51 (s, 3H), 2.84(s,3H), 7.88(d,1H), 8.31(d,1H), 8.53(s,1H); ^{13}C NMR(500 MHz, DMSO) δ 11.47, 11.64, 118.05, 123.41, 125.80, 133.28, 133.52, 148.35, 151.50, 152.49, 173.31, MS(EI): $[M+1]^+$ and $[M+1+2]^+$, m/z, 281.04, 282.04. Anal. Calcd. For $C_{11}H_9ClN_4O_3$: C, 47.07; H, 3.23; N, 19.96; Found: C, 47.11; H, 3.29; N, 19.94. (^{1}H-NMR data is shown in Figure S16, ^{13}C- NMR data is shown in Figure S23, and elemental analysis shown in Figure S35).

3,5-Dimethyl-4-(3'-nitrophenylazo) isoxazole (2b) (Fig. 12)

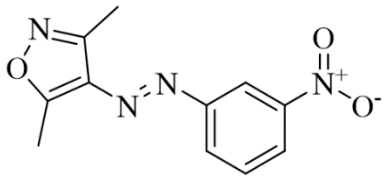

Fig. 12. 3,5-Dimethyl-4-(3′-nitrophenylazo) isoxazole

Yield: 86%; IR (ν_{max},cm^{-1}): 2923, 2856(C-H), 1603(N=N), 1491(C=C), 1405(N-O); (IR spectrum of compound in Figure S7); ^{1}H NMR(500 MHz, DMSO-d6), δ 2.50(s, 1H), 2.82 (s,3H), 7.89(dd,1H), 8.26(d,1H), 8.39(d,1H), 8.52(s,1H); ^{13}C NMR(500 MHz, DMSO) 11.14, 11.43, 112.25, 123.21, 128.12, 131.24, 134.92, 148.32, 155.50, 156.39, 163.31, MS(EI):$[M+1]^+$, m/z, 247.05. Anal. Calcd. For $C_{11}H_{10}N_4O_3$: C, 53.66; H, 4.09; N, 22.75; Found: C, 54.19; H, 4.91; N, 22.12. (^{1}H-NMR data is shown in figure-S17, mass spectrum in Figure S30).

3,5-Dimethyl-4-(2'-fluoro-4'-methylphenylazo) isoxazole (2c) (Fig. 13)

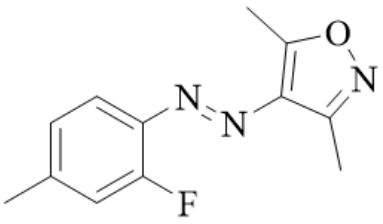

Fig. 13. 3,5-Dimethyl-4-(2′-fluoro-4′-methylphenylazo) isoxazole (2c)

Yield: 83%; IR (ν_{max},cm^{-1}): 2915, 2856(C-H), 1640(N=N), 1503(C=C), 615(C-F); (IR spectrum of compound in Figure S8); ^{1}H NMR(500 MHz, DMSO-d6) δ2.40(s,3H), 2.50(s,3H), 2.75 (s,3H), 7.10(d,1H), 7.30(d,1H), 7.6(s,1H); ^{13}C NMR(500 MHz, DMSO) δ 11.16, 11.43, 117.10, 117.25, 125.43, 132.21, 143.99, 152.72, 157.80, 159.83, 170.08; MS(EI):$[M+1]^+$, m/z, 234.12. Anal. Calcd. For $C_{12}H_{12}FN_3O$: C, 61.79; H, 5.19; N, 18.02; Found: C, 61.19; H, 4.91; N, 18.11. (^{1}H-NMR data is shown in figure-S18, ^{13}C- NMR data is shown in Figure S24, mass spectrum in Figure S31 and elemental analysis shown in Figure S36).

3,5-Dimethyl-4-(2'-fluoro-3'-chlorophenylazo) isoxazole (2d) (Fig. 14)

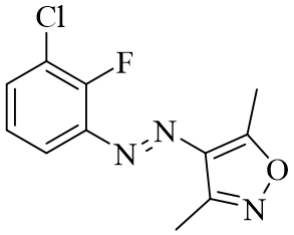

Fig. 14. 3,5-Dimethyl-4-(2′-fluoro-3′-chlorophenylazo) isoxazole (2d)

Yield: 82%; IR (ν_{max},cm^{-1}): 2976, 2861(C-H), 1570 (N=N), 1488(C=C), 608(C-F), 561(C-Cl); (IR spectrum of compound in Figure S9); ^{1}H NMR(500 MHz, DMSO-d6) δ2.45 (s, 3H), 2.78(s,3H), 7.35(d,1H), 7.65(dd,1H), 7.75(d,1H); ^{13}C NMR (500 MHz, DMSO) δ 11.35, 11.52, 117.48, 120.71, 122.91, 131.62, 149.11, 152.62, 157.14, 159.14, 170.82; MS(EI):$[M+1]^+$, $[M+1+2]^+$ m/z, 254.06, 256. 06. Anal. Calcd. For $C_{11}H_9ClFN_3O$: C, 52.09; H, 3.58; N, 16.57; Found: C, 51.90; H, 4.11; N, 16.12. (^{1}H-NMR data is shown in Figure S19, mass spectrum in Figure S32).

3,5-Dimethyl-4-(3'-chloro-4'-fluorophenylazo) isoxazole (2e) (Fig. 15)

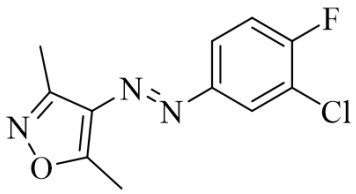

Fig. 15. 3,5-Dimethyl-4-(3′-chloro-4′-fluorophenylazo) isoxazole (2e)

Yield: 88%; IR (ν_{max},cm^{-1}): 2923, 2841(C-H), 1598 (N=N), 1496(C=C), 615(C-F), 578(C-Cl); (IR spectrum of compound in Figure S10); ^{1}H NMR(500 MHz, DMSO-d6) δ2.47(s, 3H), 2.78(s,3H), 7.60(dd,1H), 7.85(dd,1H), 8.0(dd,1H); ^{13}C NMR(500 MHz, DMSO) δ 11.25, 11.54, 117.68, 120.86, 123.64, 131.62, 149.08, 152.72, 157.34, 159.34, 170.90; MS(EI):$[M+1]^+$, $[M+1+2]^+$ m/z, 254.06, 256. 06. Anal. Calcd. For $C_{11}H_9ClFN_3O$: C, 52.09; H, 3.58; N, 16.57; Found: C, 52.12; H, 3.51; N, 17.02. (^{1}H-NMR data is shown in Figure S20, ^{13}C- NMR data is shown in Figure S25 and elemental analysis shown in Figure S37).

Biological evaluation

Anti-bacterial activity

The agar-well diffusion technique was used to evaluate the antimicrobial activity.[26] The agar plates were used to test the antibacterial activity of isolated compounds against the tested microorganisms. By using

a sterile cork borer, a plate was punched with a diameter of 6 to 8mm. Four pathogenic bacterial strains—two Gram-positive [*Staphylococcus aureus* (MTCC 96) and *Bacillus subtilis* (MTCC 121)] and two Gram-negative [*Escherichia coli* (MTCC 1652) and *Pseudomonas fluorescens* (MTCC 741)]—with a volume of 100µl inoculum were spread over the Petri plates. The diluted compound, having a concentration of up to 20 to 100 µM, was suspended inside the wells. In a BOD incubator, the plates were incubated for 24 hours at 37°C. Antibacterial activity was interpreted based on the diameter of the zone of inhibition, which was measured in millimeters (mm). The reference antibiotics used were bacitracin and chloramphenicol.

Table 1. Physiochemical properties of compound (1a-e) and (2a-e)

Code	R_1	R_2	R_3	R_4	Molecular formula	Molecular weight	Melting point	Color	Physical State
1a	-H	-H	-Br	-H	$C_9H_8BrN_5O$	282.10	152°C	brown	solid
1b	-H	-Cl	-H	-H	$C_9H_8ClN_5O$	237.65	158°C	light brown	solid
1c	-H	-H	-F	-H	$C_9H_8FN_5O$	221.20	156°C	light brown	solid
1d	-Br	-H	-H	-H	$C_9H_8BrN_5O$	282.10	148°C	yellow	solid
1e	-Cl	-H	-H	-H	$C_9H_8ClN_5O$	237.65	159°C	yellow	solid
2a	-Cl	-H	$-NO_2$	-H	$C_{11}H_9ClN_4O_3$	280.67	162°C	yellow	solid
2b	-H	$-NO_2$	-H	-H	$C_{11}H_{10}N_4O_3$	246.23	168°C	yellow	solid
2c	-F	-H	$-CH_3$	-H	$C_{12}H_{12}FN_3O$	233.25	172°C	yellow	solid
2d	-F	-Cl	-H	-H	$C_{11}H_9ClFN_3O$	253.66	178°C	yellow	solid
2e	-H	-Cl	-F	-H	$C_{11}H_9ClFN_3O$	253.66	170°C	yellow	solid

Anti-oxidant activity by DPPH radical scavenging assay

The *in vitro* antioxidant potential of synthesized compounds was evaluated using the 1,1-diphenyl-2-picryl hydrazide (DPPH) radical scavenging method.[27] For the stock solution, a total of 24 mg of DPPH was dissolved in 100 ml of ethanol. Ethanol filtering of the DPPH stock solution produced an effective combination with an absorbance of about 0.973 at 517 nm. Used a 3 mL DPPH solution, and introduced 100 µl of varying concentrations of the test compound (20, 40, 60, 80, and 100 µM) in ethanol. After 30 minutes of rt incubation, the absorbance was measured at 517 nm against a blank.

The percentage inhibitions were calculated using the following formula: DPPH scavenging activity (%)

$$= \frac{[(A_{control}\text{-}A)] \times 100}{A_{control}}$$

where A is the absorbance of the test compound and $A_{control}$ is the absorbance of the control reaction (which contains all the reagents save the test compound).

Anti-cancer activity

Materials

Fetal Bovine Serum (FBS), Dulbecco's Modified Eagle Medium (DMEM), Roswell Park Memorial Institute (RPMI)-1640 medium, and antibiotic solutions (100 units/ml penicillin and 10 µM streptomycin) were provided by HiMedia Laboratories Pvt. Ltd., Mumbai, India. MTT [3-(4,5-dimethylthiazol-2-yl)-2,5-diphenyl tetrazolium bromide] and all other chemical and reagent with analytical grade were used in different experiments.

Cell culture

The PC3 cell line (derived from a metastatic site: bone) representing human prostate cancer and human embryonic kidney (HEK-293) cells were procured from the National Centre for Cell Science (NCCS) located in Pune, India. PC-3 cells were nurtured in RPMI-1640 medium, while HEK-293 cells were cultivated in DMEM supplemented with 10% FBS and 1% penicillin-streptomycin antibiotic solution. Cells were grown at 37°C in a 5% CO_2 culture condition.

Drug treatment

The stock solutions of various compounds at a concentration of 1M were prepared using DMSO as the solvent. The initial stock was further diluted into millimolar concentrations, and the ultimately specified final concentration for cell treatment was directly diluted into the culture media. For vehicle control, 0.1% DMSO in media was used.

MTT [3-(4,5-Methylthiazol-2-yl)-2,5-diphenyl-tetrazolium bromide] assay

The cytotoxicity of different substances on normal human embryonic kidney (HEK) and prostate cancer (PC3) cells was assessed using the MTT assay. In 96-well plates, cells were seeded at a density of 2.5×10^3 for 24 hours and then left to re attach for another 24 hours. Different chemical concentrations, ranging from 5 µM to 640 µM, were applied to the cells. The media was changed after the treatment period of 24 hours to new media containing 100 µg of MTT per well, and it was incubated for 4 hours at 37°C.

After the removal of the media, to dissolve the purple formazan crystal, 100 µL of DMSO was added to each well. The absorbance was measured at 595 nm using an ELISA reader (Bio-Rad). Cell viability was calculated by using the following formula:

$$\textbf{\% cell viability} = \frac{\mathbf{A_{treated}\text{-}A_{blank}}}{\mathbf{A_{control}\text{-}A_{blank}}} \times \mathbf{100}$$

Statistical analysis

GraphPad prism 8 [GraphPad software, Inc., La Jolla. GA] was used for statistical analysis. Ordinary One-way ANOVA [Analysis for variance] was employed

for checking the statistical significance of the results. All sample were analyzed in triplicate and expressed as mean± SD for n=3. The p value determined the level of significance at different. The p<0.0001 (****) were regarded as highly significant.

Results and discussion

Chemistry

The synthetic pathways selected for the preparation of key intermediates, 2-[(substituted phenyl)hydrazono]malononitrile (1) and 3-[(substituted phenyl) azo]-2,4-pentanedione (2), as well as the target compounds (1a-e) and (2a-e), are outlined in Figure 3, with Figures 4 and 5 illustrating the mechanisms of the synthetic paths. In Figure 3, the reaction of 2-[(substituted phenyl)hydrazono]malononitrile (1) and 3-[(substituted phenyl)azo]-2,4-pentanedione (2) with hydroxylamine hydrochloride and sodium acetate in a 1:1 ratio yielded isoxazoles (1a-e) and (2a-e) in good yields (75-91%). The infrared (IR) spectrum of the novel isoxazole analogues (1a-e) and (2a-e) revealed distinctive absorption bands indicative of specific functional groups. Notably, the NH_2 groups exhibited symmetric stretching at 3397 cm^{-1} and asymmetric stretching at 3264 cm^{-1}, while the CH_3 groups demonstrated symmetric stretching at 2915 cm^{-1} and asymmetric stretching at 2896 cm^{-1}. These absorption peaks provided valuable insights into the molecular composition and structural characteristics of the compounds under investigation. The stretching frequency resulting from the azo group gave rise to a prominent absorption band in the range of 1410 to 1490 cm^{-1}, while absorption bands associated with C=C stretching manifested within the range of 1610 to 1632 cm^{-1}.

The disappearance of two singlet peaks in compounds (1a-e) and the emergence of two singlet peaks at δ 6.12-8.51 ppm, corresponding to two NH_2 protons, were confirmed by the ^1H NMR and D_2O exchangeable spectra of the respective isoxazoles. In the new isoxazole ring (2a-e), two substituted methyl groups appeared as singlet peaks, each representing three protons with intensity at δ 2.45-2.84 ppm in the ^1H NMR spectra. All compounds exhibited a proton signal in the range of δ 7.11 to 8.52 ppm for the substituted phenyl ring with various functional groups. Additionally, the ^{13}C NMR spectra of (1a-e) and (2a-e) were observed in the range of δ 105.12-173.12, with methyl carbon in (2a-e) appearing at δ 11.16-11.64 ppm.

Antibacterial activity assessment

The results revealed that all the compounds exhibited a moderate level of antibacterial activity against the four tested pathogenic bacterial strains *B. subtilis* (MTCC 121) and *S. aureus* (MTCC 96), *P. fluorescens* (MTCC 741) and *E. coli* (MTCC 1652). Compound 2a demonstrated the highest level of activity against *E. coli* (20 mm), compound 1d demonstrated the lowest level of activity against *P. fluorescens* (11 mm), and compound 1e demonstrated the least amount of activity against *B. subtilis*. There was no evidence of inhibition observed in the negative control (DMSO). All the compounds showed significant inhibition of growth in the tested microorganisms at a concentration of 100 µM. The potency of all compounds was compared with the reference drugs bacitracin and chloramphenicol. Bacitracin exhibited the largest zone of inhibition at 28 mm against both *P. fluorescens* and *E. coli*. Meanwhile, chloramphenicol demonstrated the highest zone of inhibition at 30 mm, particularly against *E. coli*. Table 2 indicates the zone of inhibition, while Figure 16 illustrates the antibacterial activity graph of compounds (1a-e) and (2a-e).

Table 2. Zone of inhibition of antibacterial activity of compound (1a-e) and (2a-e)

	Gram positive bacteria		Gram negative bacteria	
	B. subtilis	*S. aureus*	*P. fluorescens*	*E. coli*
Compound	Zone of inhibition (mm)	Zone of inhibition (mm)	Zone of inhibition (mm)	Zone of inhibition (mm)
1a	14.14±0.16	18.11±0.16	12.25±0.34	17.14±0.16
1b	13.15±0.19	13.14±0.16	16.22±0.22	12.16±0.20
1c	16.22±0.24	16.18±0.21	12.36±0.34	17.16±0.24
1d	12.17±0.22	14.16±0.19	11.33±0.40	18.21±0.26
1e	11.23±0.27	14.16±0.21	12.25±0.29	16.17±0.26
2a	16.26±0.29	18.20±0.31	14.32±0.29	20.14±0.17
2b	19.24±0.27	15.25±0.29	15.32±0.34	16.22±0.21
2c	15.17±0.19	14.18±0.19	12.43±0.48	15.14±0.16
2d	14.2±0.25	15.22±.29	14.22±0.29	18.13±0.14
2e	16.21±0.21	14.26±0.29	16.43±0.38	19.15±0.18
Bacitracin	25.16±0.20	26.18±.24	28.34±0.35	28.18±0.26
Chloramphenicol	26.13±0.16	23.25±0.37	27.44±0.44	30.18±0.19

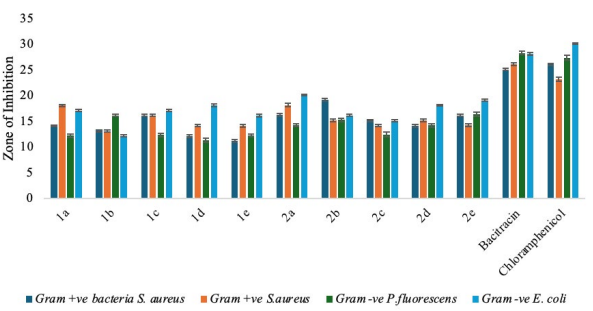

Fig. 16. Antibacterial activity graph of isoxazole derivative (1a-e) & (2a-e). Data are means ± SD from three independent experiments

Antioxidant activity

The newly synthesized compounds were also evaluated for their antioxidant properties using 1,1-diphenyl-2-picryl hydrazide (DPPH). All the compounds exhibited good radical-scavenging activity, but compounds 1d, 1e, 2c, 2d, and 2e demonstrated a particularly strong range of radical scavenging activity at the

concentration of 20, 40, 60, 80,100 µM compared to the others (Fig. 17). The percentage of DPPH activity, calculated using the reported formula, was 33.19%, 22.23%, 36.51%, 28.22%, and 36.04%, respectively. Color variations were observed in the tested compounds after a 30-minute incubation with a DPPH-containing solution. Figure 17 illustrates the antioxidant activity graph of the isoxazole derivatives (1a-e) and (2a-e).

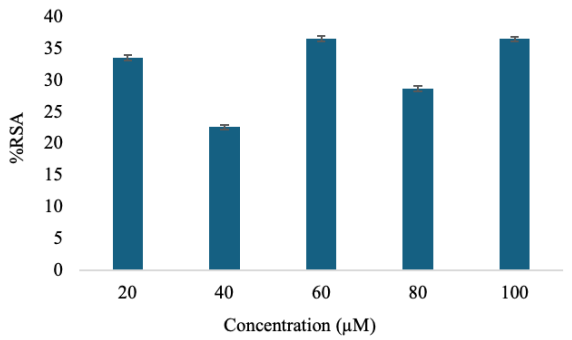

Fig. 17. Anti-oxidant activity graph of isoxazole derivative (1a-e) & (2a-e). Data are means ± SD from three independent experiments

Anticancer activity

Compounds 1a, 1b, 1c, and 1d were assessed for their anticancer activity against PC3 and HEK cell lines at various concentrations ranging from 10 µM to 640 µM, among all the synthesized compounds. Across different dosages of drug treatments, these tested compounds consistently demonstrated greater inhibition of cancer cell lines compared to normal cells (Figures 18-21). Notably, these compounds exhibited their maximum inhibitory effect on normal cells only at higher doses, specifically at 640 µM, while demonstrating an effect on cancer cell lines at lower doses. The IC_{50} values of compounds 1a, 1b, 1c, and 1d are presented in Table 3.

Table 3. The IC_{50} value of compound 1a, 1b, 1c, and 1d

Compound	IC_{50} (µM)	
	PC3	HEK
(1a) 3, 5-Diamino-4-(4′-bromophenylazo) isoxazole 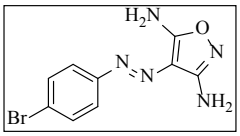	53.96±1.732	41.24±1.881
(1b) 3, 5-Diamino-4-(3′-chlorophenylazo) isoxazole 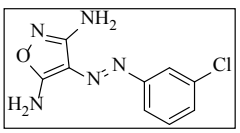	47.27±1.675	42.10±1.46
(1c) 3, 5-Diamino-4-(4′-fluorophenylazo) isoxazole 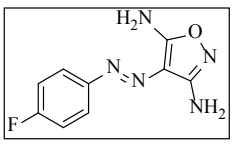	147.9±2.170	66.13±2.073
(1d) 3,5-Diamino-4-(2′-bromophenylazo) isoxazole 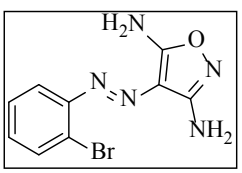	38.63±1.587	103.1±1.900
Doxorubicin	0.09±0.014	171.65±2.65

SAR analysis

The isoxazole heterocycle exhibits significant pharmacological activities, particularly as an anticancer agent, as highlighted in recent research findings concerning this fundamental structure.[28] This observation is corroborated by evidence that the isoxazole heterocycle serves as a crucial pharmacophore for antiproliferative activities. Furthermore, the effectiveness of these activities is notably enhanced when the phenyl ring is substituted with halogens, specifically fluorine (F), bro-

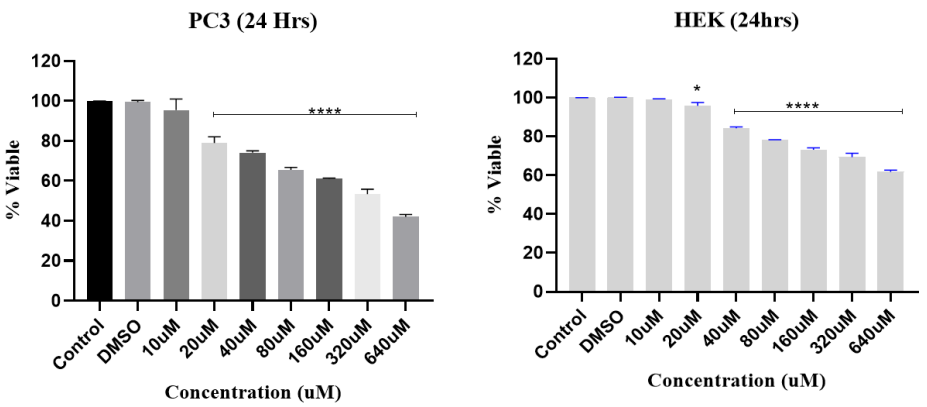

MTT assay showing dose-dependent decrease in cell viability of PC3 cells after 24hrs of treatment. Data are means ± SD from two independent experiments, (****p<0.0001) with respect to untreated control. Differences between groups were analysed by one way ANOVA.

MTT assay showing dose-dependent decrease in cell viability at higher doses on HEK cells after 24hrs of treatment. Data are means ± SD from two independent experiments, (*p=0.0161, ****p<0.0001)) with respect to untreated control. Differences between groups were analysed by one way ANOVA.

Fig. 18. Effect of different doses of 1a compound on cell viability of prostate cancer; and effect of different doses of 1a compound on cell viability of normal human embryonic kidney cells (HEK)

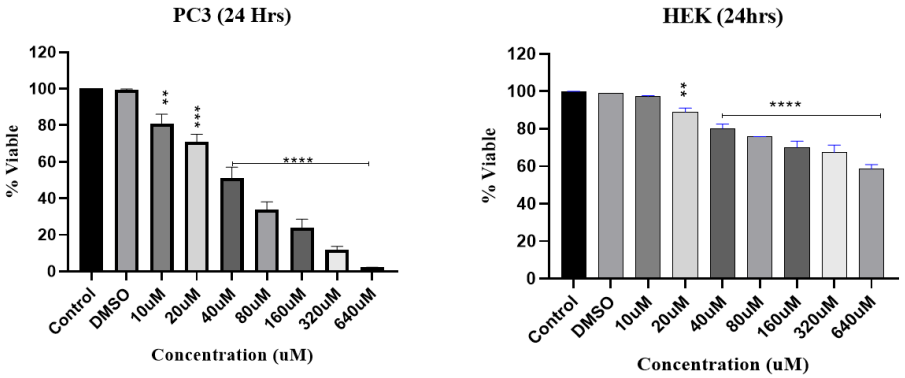

MTT assay showing dose-dependent decrease in cell viability of PC3 cells after 24hrs of treatment. Data are means ± SD from two independent experiments, (**p=0.0030, ***P=0.0001 ****p<0.0001) with respect to untreated control. Differences between groups were analysed by one way ANOVA.

MTT assay showing dose-dependent decrease in cell viability at higher doses on HEK cells after 24hrs of treatment. Data are means ± SD from two independent experiments, (**p=0.0042, ****≤p=0.0001) with respect to untreated control. Differences between groups were analysed by one way ANOVA.

Fig. 19. Effect of different doses of 1b compound on cell viability of prostate cancer; and effect of different doses of 1b compound on cell viability of normal human embryonic kidney cells (HEK)

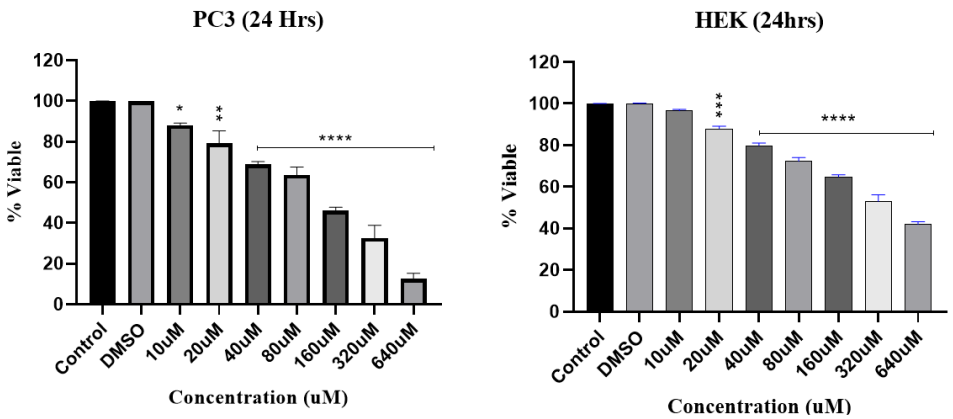

MTT assay showing dose-dependent decrease in cell viability of PC3 cells after 24hrs of treatment. Data are means ± SD from two independent experiments, (*P=0.0372 **P=0.0011, ****p<0.0001) with respect to untreated control. Differences between groups were analysed by one way ANOVA.

MTT assay showing dose-dependent decrease in cell viability at higher doses on HEK cells after 24hrs of treatment. Data are means ± SD from two independent experiments, (***P=0.0001, ****p<0.0001) with respect to untreated control. Differences between groups were analysed by one way ANOVA.

Fig. 20. Effect of different doses of 1c compound on cell viability of prostate cancer; and effect of different doses of 1c compound on cell viability of normal human embryonic kidney cells (HEK)

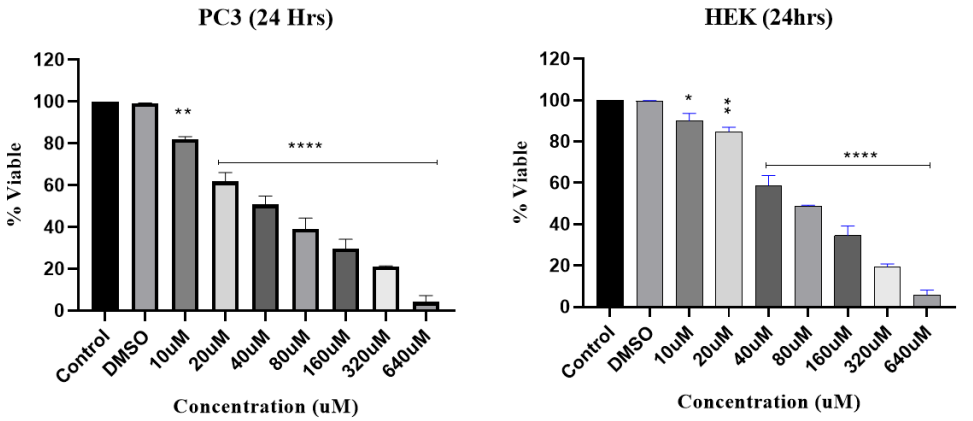

MTT assay showing dose-dependent decrease in cell viability of PC3 cells after 24hrs of treatment. Data are means ± SD from two independent experiments, (**p=0.0019, ****p<0.0001) with respect to untreated control. Differences between groups were analysed by one way ANOVA.

MTT assay showing dose-dependent decrease in cell viability at higher doses on HEK cells after 24hrs of treatment. Data are means ± SD from two independent experiments, (*P=0.0295, **P=0.0022, ****p<0.0001) with respect to untreated control. Differences between groups were analysed by one way ANOVA.

Fig. 21. Effect of different doses of 1d compound on cell viability of prostate cancer; and effect of different doses of 1d compound on cell viability of normal human embryonic kidney cells (HEK)

mine (Br), and/or chlorine (Cl).[29-30] In our study, all analogues with electron withdrawing groups such as -F, -Cl, and -Br demonstrated anticancer effects against experimental cancer cell lines. Among these, in the PC3 cell line, the ortho-substituted analogue 1d exhibited the most potent cytotoxic effects, followed by the meta-substituted 1b and then the para-substituted 1a and 1c. Among the para-substituted analogs, 1a and 1c, the bromine-substituted analogue showed greater cytotoxic effects compared to the fluorine-substituted analogue. In the HEK cell line, the para-substituted analogue 1a showed superior anticancer effects compared to the meta-substituted 1b, followed by the ortho-substituted 1d. However, among the para-substituted analogs, 1a and 1c, the bromine-substituted analogue demonstrated greater cytotoxic effects compared to the fluorine-substituted analogue, similar to what was observed in the PC3 cell line. It appears that the size, position, and electronic effects of the substituents play an important role in determining activity.

Conclusion

In the pursuit of novel compounds with multifaceted biological activity, we have successfully devised and validated a synthetic route to produce isoxazole derivatives (1a-e) and (2a-e). Rigorously scrutinized through diverse spectral analyses, this synthetic pathway has been validated. Moving beyond synthesis, we embarked on a comprehensive journey to unravel the potential biological attributes of these compounds. Our investigations encompassed a holistic evaluation of antibacterial, antioxidant, and anticancer properties. In terms of antibacterial prowess, all compounds emerged as robust contenders against both Gram-positive and Gram-negative bacterial strains. Notably, compound 2a exhibited maximum activity against *E. coli*. Compounds 1d, 1e, 2c, 2d, and 2e demonstrated a good range of radical scavenging activity compared to other compounds. The percentage of DPPH activity calculated using the reported formula was 33.19%, 22.23%, 36.51%, 28.22%, and 36.04%, respectively. Compounds 1b, 1c, and 1d exhibited greater anticancer potential against PC3 cell lines at a dose of 640 μM of drug treatment, with 1d also demonstrating excellent potential and effect against the cell viability of HEK cell lines. The synthetic route can be further optimized to enhance efficiency, reduce costs, or explore variations in the chemical structure to improve the overall synthetic process. Furthermore, we can delve deeper into the structure-activity relationship of these compounds to understand the specific structural features responsible for their biological activities. This knowledge can guide the design of new derivatives with improved efficacy.

The potential of isoxazole derivatives is rich with promise, spanning a diverse array of therapeutic applications within medicine and beyond. The future prospects of isoxazole in the development of antibacterial and anticancer drugs entail further exploration of their mechanisms of action, optimization of their pharmacokinetic properties, and rigorous preclinical and clinical evaluations. Given the global health threat posed by multidrug-resistant bacteria, isoxazole derivatives could provide a new avenue for combating bacterial infections. Additionally, their potential as anticancer agents open doors to innovative and targeted cancer treatments, instilling hope for improved therapeutic outcomes in the battle against both infectious diseases and cancer.

Acknowledgments

The authors express gratitude to all members of the Chemistry Department at Maharishi Markandeshwar (Deemed to be university) for their invaluable support, assistance, and encouragement throughout the course of this research. We are also thankful to Department of Bio-sciences and Technology, Maharishi Markandeshwar (Deemed to be university) for biological activity tests.

Declarations

Funding

Financial support from the MM (DU) Education Trust management is available to facilitate the execution of this research.

Author contributions

Conceptualization, P.S. and A.B.; Methodology, K.V.; Software, T.S.; Validation, T.S., R.K. and H.T.; Formal Analysis, K.V.; Investigation, P.S.; Resources, P.S.; Data Curation, K.V.; Writing – Original Draft Preparation, K.V.; Writing – Review & Editing, P.S.; Visualization, A.B.; Supervision, P.S.

Conflict of interest

The authors state, there are no conflict of interest about the publication of this research work.

Data availability

The dataset generated during research work is available from corresponding author on request.

Ethics approval

Not applicable.

References

1. Doron S, Gorbach SL. Bacterial infections: overview. *International Encyclopedia of Public Health*. 2008:273. doi: 10.1016/B978-012373960-5.00596-7
2. Ma M, Cheng Y, Xu Z, et al. Evaluation of polyamidoamine (PAMAM) dendrimers as drug carriers of anti-bacterial drugs using sulfamethoxazole (SMZ) as a model

drug. *Eur J Med Chem*. 2007;42(1):93-98. doi: 10.1016/j.ejmech.2006.07.015
3. Yanagihara K. Design of anti-bacterial drug and anti-mycobacterial drug for drug delivery system. *Curr Pharm Des*. 2002;8(6):475-482. doi: 10.2174/1381612023395808
4. Diana P, Carbone A, Barraja P, Kelter G, Fiebig H, Cirrincione G. Bioorganic & Medicinal Chemistry and 3 , 5-bis (3 0 -indolyl) -isoxazoles , nortopsentin analogues. *Bioorg Med Chem*. 2010;18(12):4524-4529. doi: 10.1016/j.bmc.2010.04.061
5. Sethi P, Khare R, Choudhary R. Complexes of pyrimidine thiones: Mechanochemical synthesis and biological evaluation. *Asian J Chem*. 2020;32(10):2594-2600. doi: 10.14233/ajchem.2020.22813
6. Pooja S, Pernita D, Gupta GK, Mostafa Sahar I, Simrat K. Synthesis, characterization, anti-bacterial and DNA nicking activity of new complexes of 1-(2,4-dinitrophenylamino)- 4, 4, 6-trimethyl-3, 4-dihydropyrimidine-2-(1H)--thione. *Res J Chem Environ*. 2018;22(11):73-88.
7. Joseph L, George M. Evaluation of in vivo and in vitro anti-inflammatory activity of novel isoxazole series. *Eur Int J Sci Technol*. 2016;5(3):35-42.
8. Mączyński M, Artym J, Kocięba M, Kochanowska I, Ryng S, Zimecki M. Anti-inflammatory properties of an isoxazole derivative - MZO-2. *Pharmacol Reports*. 2016;68(5):894-902. doi: 10.1016/j.pharep.2016.04.017
9. Huang X, Dong S, Liu H, et al. Design, Synthesis, and Evaluation of Novel Benzo [d] isoxazole Derivatives as Anticonvulsants by Selectively Blocking the Voltage--Gated Sodium ChannelNaV1.1. *ACSChemNeurosci*. 2022;13(6):834-845.doi: 10.1021/acschemneuro.1c00846
10. Hawash M, Jaradat N, Abualhasan M, et al. Evaluation of cytotoxic, COX inhibitory, and antimicrobial activities of novel isoxazole-carboxamide derivatives. *Lett Drug Des Discov*. 2023;20(12):1994-2002. doi: 10.2174/1570180819666220819151002
11. Pir M, Agirbas H, Budak F, Sahin O. Synthesis, characterization, antimicrobial activity, and QSAR studies of some new 6-substituted phenyl 3-(4-chlorophenyl)-3a,4,8,8a-tetrahydro-[1,3,2]dioxaborepino [5,6-d]isoxazoles. *Heteroat Chem*. 2017;28(2):1-12. doi: 10.1002/hc.21363
12. Saravanan G, Alagarsamy V, Dineshkumar P. Synthesis, analgesic, anti-inflammatory and in vitro antimicrobial activities of some novel isoxazole coupled quinazolin-4 (3 H)-one derivatives. *Arch Pharm Res*. 2021;44:1-11. doi: 10.1007/s12272-013-0262-8
13. Shahinshavali S, Sreenivasulu R, Guttikonda VR, Kolli D, Rao MVB. Synthesis and Anticancer Activity of Amide Derivatives of 1,2-Isoxazole Combined 1,2,4-Thiadiazole. *Russ J Gen Chem*. 2019;89(2):324-329. doi: 10.1134/S1070363219020257
14. Burra S, Voora V, Rao CP, Vijay Kumar P, Kancha RK, David Krupadanam GL. Synthesis of novel forskolin isoxazole derivatives with potent anti-cancer activity against breast cancer cell lines. *Bioorganic Med Chem Lett*. 2017;27(18):4314-4318. doi: 10.1016/j.bmcl.2017.08.033
15. Hawash M. Recent advances of tubulin inhibitors targeting the colchicine binding site for cancer therapy. *Biomolecules*. 2022;12(12):1843. doi: 10.3390/biom12121843
16. Hawash M, Jaradat N, Eid AM, et al. Synthesis of novel isoxazole–carboxamide derivatives as promising agents for melanoma and targeted nano-emulgel conjugate for improved cellular permeability. *BMC Chem*. 2022;16(1):1-12. doi: 10.1186/s13065-022-00839-5
17. Shaik A, Bhandare RR, Palleapati K, Nissankararao S, Kancharlapalli V, Shaik S. Antimicrobial, antioxidant, and anticancer activities of some novel isoxazole ring containing chalcone and dihydropyrazole derivatives. *Molecules*. 2020;25(5):1047. doi: 10.3390/molecules25051047
18. Chithra VS, Reji TF, Brindha J. Synthesis and Structure--Activity Relationship Study of Novel Isoxazole derivatives as Promising Antioxidants. *Asian J Res Chem*. 2018;11(1):65-68. doi: 10.5958/0974-4150.2018.00014.7
19. Ketan V, Pooja S, Purti M, Anshul B. Antituberculosis activity of pyrazoles. *Res J Chem Environ*. 2022;26(10):184-198. doi: 10.25303/2610rjce1840198
20. Abdul Manan MAF, Cordes DB, Slawin AMZ, et al. The Synthesis and Evaluation of Fluoro-, Trifluoromethyl-, and Iodomuscimols as GABA Agonists. *Chem - A Eur J*. 2017;23(45):10848-10852. doi: 10.1002/chem.201701443.
21. Rahman MU, Rathore A, Siddiqui AA, Parveen G, Shahar Yar M. Synthesis and antihypertensive screening of new derivatives of quinazolines linked with isoxazole. *Biomed Res Int*. 2014;2014. doi: 10.1155/2014/739056.
22. Agrawal N, Mishra P. Synthesis, monoamine oxidase inhibitory activity and computational study of novel isoxazole derivatives as potential antiparkinson agents. *Comput Biol Chem*. 2019;79:63-72. doi: 10.1016/j.compbiolchem.2019.01.012.
23. Pedada SR, Yarla NS, Tambade PJ, et al. Synthesis of new secretory phospholipase A2-inhibitory indole containing isoxazole derivatives as anti-inflammatory and anticancer agents. *Eur J Med Chem*. 2016;112:289-297. doi: 10.1016/j.ejmech.2016.02.025.
24. Aggarwal R, Bansal A, Mittal A. Synthesis and antimicrobial activity of 3-(2-thienyl)-4-arylazo--5-hydroxy- 5-trifluoromethyl-Δ2-isoxazolines and 3-(2-thienyl)-4-arylazo- 5-trifluoromethylisoxazoles. *J Fluor Chem*. 2013;145(2010):95-101. doi: 10.1016/j.jfluchem.2012.10.005.
25. Kryštof V, Cankař P, Fryšová I, et al. 4-Arylazo-3 , 5-diamino-1 H -pyrazole CDK Inhibitors : SAR Study , Crystal Structure in Complex. *J Med Chem*. 2006;49(22):6500-6509. doi: 10.1021/jm0605740.
26. Perez C. Antibiotic assay by agar-well diffusion method. *Acta Biol Med Exp*. 1990;15:113-115.
27. Garcia EJ, Oldoni TLC, Alencar SM de, Reis A, Loguercio AD, Grande RHM. Antioxidant activity by DPPH assay of potential solutions to be applied on bleached teeth. *Braz Dent J*. 2012;23:22-27. doi: 10.1590/S0103-64402012000100004.

28. Arya GC, Kaur K, Jaitak V. Isoxazole derivatives as anticancer agent: A review on synthetic strategies, mechanism of action and SAR studies. *Eur J Med Chem*. 2021;221:113511. doi: 10.1016/j.ejmech.2021.113511.
29. Hawash M, Jaradat N, Bawwab N, Salem K, Arafat H. Design, synthesis, and biological evaluation of phenyl - isoxazole - carboxamide derivatives as anticancer agents. *Heterocyclic Communications*. 2021:133-141. doi: 10.1515/hc-2020-0134
30. Hawash M, Kahraman DC, Ergun SG, Cetin-Atalay R, Baytas SN. Synthesis of novel indole-isoxazole hybrids and evaluation of their cytotoxic activities on hepatocellular carcinoma cell lines. *BMC Chem*. 2021;15(1):1-14. doi: 10.1186/s13065-021-00793-8